Allosteric transitions of proteins studied by topological networks: a preliminary investigation on human haemoglobin.

Lisa Beatrice Caruso [1], **Alessandro Giuliani** [2] **Alfredo Colosimo**[1]
Dept. of Anatomy, Histology, Forensic Medicine and Orthopaedics
Sapienza, University of Rome [1]
Environment and Health Dept. , Istituto Superiore di Sanitá, Rome, Italy[2]

Keywords: Hemoglobin, Biological Networks, Allosteric mechanisms

Abstract: A concise description of the 3D structure of α and β chains of human haemoglobin, as well as of αβ dimers, is provided for both the R and T forms on the basis of topological network parameters. Such parameters are able to account for the allosteric conformational transitions as derived by standard 3D pictures and models in the literature. In particular, the difference between the R and T forms appears more relevant in the case of dimers, in agreement with the idea that dimers are essential in the allosteric mechanism of Hb as an oxygen carrier. This result encourages the extension of the network-based, topological representation of protein structures to less overexploited systems than Hb, as well as to the vast realm of data coming from resonance spectroscopy.

1 INTRODUCTION

Allostery is a complex process by which the global functional properties of biological molecules are controlled through ligand binding events. Allosteric models provide mechanisms accounting for the interactions between distant binding sites mediated by shifting the equilibrium of the whole molecule between different structural conformations.

Any mechanistic description of the sigmoidal shape of the 0_2-binding curve of Hb somehow oscillates in between the two extreme cases of allosteric models, namely the "concerted" Monod-Wyman-Changeux (MWC) model [1] and the "sequential" Koshland-Nemethy-Filter (KNF) model [2]. The former assumes an all-or-none change in the quaternary structure, whereas the latter allows for a sequence of structural changes transferred from one subunit to another. Although both models were proposed many years ago, as a matter of fact their possible refinements are still under discussion [3], [4] .

For most allosteric proteins knowledge of the X-ray crystal structures of the 100% T (ligand-free) and 100% R (ligand-bound) states was extremely precious to understand the allosteric changes [5–9]. It is worth remembering, however, that by comparison of the static pictures provided by R and T tertiary structures (see Figure 1), even at the highest possible resolution, no final conclusion concerning the underlying mechanisms can be drawn.

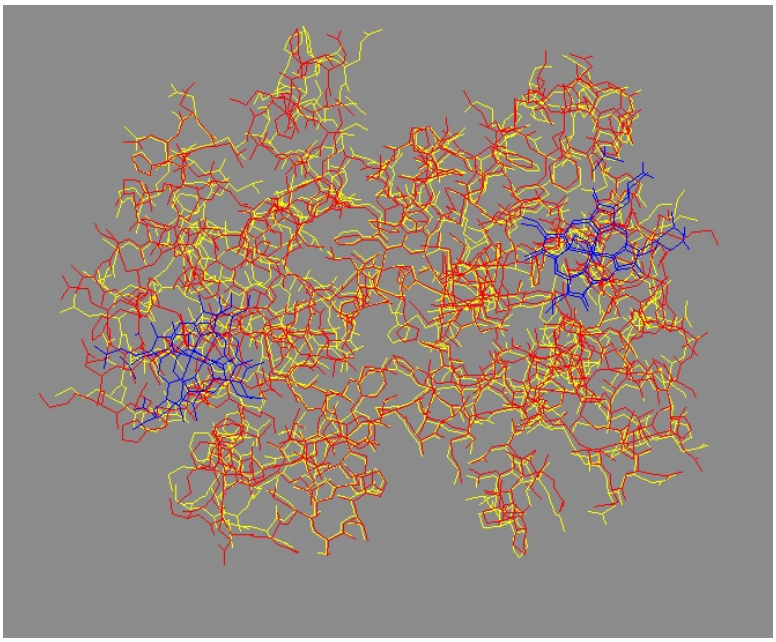

Figure 1: ***G****eometrical difference between allosteric conformation of the* α *and* β *Hb chains.*
The R (yellow) and the T (red) conformations of the αβ dimer of human Hb, have been superimposed by minimizing the RMSD (Root Mean Square Deviation) value. Even under the best overlapping condition (RMSD = 0.82 $\AA$) the picture does not authorize any conclusion concerning the switching mechanism.

Notwithstanding the common experimental basis, a topological representation of protein structures inspired by the graph theory [10] may result easier to analyze in mechanistic terms than the classical 'geometrical' picture, at least in so far as the main emphasis is given to the changing landscape of between residues contacts. In particular, the identification of 'allosteric hot spots' as the residues most involved in the allosteric transition could be of great help in designing 'allosteric drugs', i.e. molecules trying to modulate allosteric properties of their target that were hypothesized to act as 'network modulators', so overcoming a major problem of nowadays pharmacology [11].

In this report we concentrate on the representation of protein 3D structures by means of networks of nodes (aminoacids) whose chemical interactions (of any type, both covalent and non-covalent) are reduced to links between nodes. This type of representation of protein structures has been used in many fields, like protein folding [12] and the prediction of functionally important residues in some families of enzymes [13] and proteins [14, 15]. However, at our best knowledge, only in a very limited number of cases it has been used, up to now, in the study of allosteric mechanisms [15].

The first part of this report summarizes the basics of the network representation of protein 3D data, including the calculation of global network parameters in a simple case. The following part summarizes the results obtained in the comparison of network parameters from isolated chains and αβ dimers of human haemoglobin in different allosteric conformations. The network approach is finally discussed as potentially useful in designing new mechanistic models or in resolving the controversial ones.

2 MATERIALS AND METHODS

A recently implemented database constituting a great resource for searching, viewing and analyzing structures and functions of allosteric molecules is the ASD [16], AlloSteric Database (http://mdl.shsmu.edu.cm/ASD/). This database is actually updated every 6 months and contains at the moment (January 2012), 336 allosteric proteins from 101 species and 8095 modulators. For each molecule reference to other databases such as PubMed (http://www.ncbi.nlm.nih.gov/pubmed/) and UniProt (http://www.uniprot.org/) is also provided. We analyzed the T and R conformations of human haemoglobin (Figure 1), since the structural rearrangement occurring in switching from one to the other has been the subject of plentiful experimental and modelistic studies. Based on the literature data we represented such conformations from a topological point of view to check up to what point it was possible to enlight the details of the conformational switch.

The normal adult haemoglobin consists of four subunits having a similar 3D structure, two identical α chains (141 amino acids) , and two identical β chains (146 amino acids) . Each subunit has a haeme pocket where the 0_2 binds Fe^{2+}. The transition from the low-affinity form (T, tense) to high affinity (R, relaxed) of haemoglobin as a consequence of oxygen binding [17] is one of the most studied allosteric processes.

3D (geometrical) versus Network (topological) representation of haemoglobin

The three-dimensional structures of the T and R forms of haemoglobin were obtained from the Protein Data Bank (http://www.rcsb.org/pdb/home/home.do) as 1gbv and 1aj9 files, respectively. Displaying 3D structures from PDB files can be obtained by several graphics programs. Among these PDB Viewer allows, in the case of multimeric proteins, to isolate each single subunit from the others. Thus, we could perform a calculation of the RMSD of the α and β subunits of haemoglobin in the T and R form, in order to quantify their overlapping (Figure 2) and pick up the individual residues with a critical role in the allosteric rearrangement.

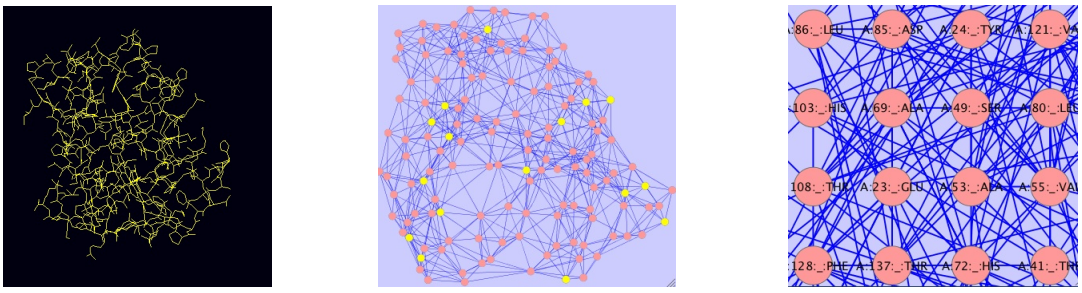

Figure 2: ***G**eometric and topological representation of a protein structure.*
The left and middle panels refer to the α chain of human haemoglobin (PDB file = 1gbv) in the standard 3D, and topological (network) structure, respectively. The right panel shows an amplified 2D picture of a selected number of nodes (yellow in the middle panel) from the 3D picture. The number associated to each node indicates the location of the corresponding residue in the primary structure. The "links" among residues are defined on the basis of a threshold distance of 5 $\AA$.

The topological representation of the T and R forms of haemoglobin was generated using RING (Residue Interaction Network Generator) [18], a software tool useful to draw the network of chaemical interactions (links) among amino acid residues. From the 3D coordinates in the PDB file a link between a couple of residues is drawn if the distance between any pair of atoms each pertaining to one member of the couple is lower than a predefined threshold. In our case we checked that, making more restrictive the default threshold (5 $\AA$), namely decreasing the value to 4 $\AA$ and 3 $\AA$, the overall topological picture didn't change significantly.

Once the whole grid of links is calculated, the network can be characterized, through the evaluation of quantitative descriptors, and observed using Cytoscape, an open source software platform for visualizing molecular

interactions and biological pathways [19–21].

The main parameters considered in our work together with their meaning are detailed in the following list (for a concise analytical definition of the parameters see Table 1):

Name	*Definition*
Node degree/connectivity (k_i)	# of links of node i
Node degree distribution	# of nodes with degree k (k = 0, 1, 2, ...)
Clustering coefficient	undirected graphs: $C_i = \frac{2e_i}{k_i(k_i-1)}$ k_i: # of neighbors (links) of node i e_i: # of connected pairs within all neighbors of node i
Shortest path length	between nodes i and j: L_{ij}
Network diameter	maximum length of shortest paths between two nodes
Characteristic path length	CPL: average of the shortest paths between two nodes
Network Density	$\frac{mean(k)}{n-1}$
Centralization	$\frac{n}{n-2}(\frac{max(k)}{n-1}$ - Density)
Network heterogeneity	$\frac{\sqrt{variance(k)}}{mean(k)}$: tendency of a network to include hub nodes

Table 1: *Name and definition of the network parameters used in this work.*

Node degree. The degree or connectivity (k), is the most elementary characteristic of a node, namely how many links connect the node to other nodes. In directed graphs, the in-degree of a node is the number of incoming edges and the out-degree is the number of outgoing edges. In this work we considered undirected graphs, so the node degree simply corresponds to the number of links in which a specific node is involved.

Node degree distribution. Barábasi and Albert used the node degree distribution to distinguish between random [22] and scale-free network topologies [10].The degree distribution allows to distinguish between different classes of networks. Protein networks were demonstrated to lay between scale-free and random graphs in which several highly connected clusters are separated from each other by structural cavities [23].

Clustering coefficient. In both directed and undirected graphs, the clustering coefficient is a number between 0 and 1 giving the ratio N/M, where N is the number of links between neighbors of the i_{th} node, and M is the maximum number of links that could possibly exist between the neighbors of the i_{th} node. In directed graphs the clustering coefficient value is halved. The average clustering coefficient distribution gives the average of the clustering coefficients for all nodes with k neighbors, with k >= 2,.

Shortest path. The length of the shortest path between two nodes n and m is $L_{n,m}$. The shortest path length distribution gives the number of node pairs (n,m) with $L_{n,m}$ = k, for k = 1,2, .

Network diameter. The network diameter is the maximum of shortest path values between all couples nodes. If a network is disconnected, its diameter is the maximum of all diameters of its connected components. The network diameter and the shortest path length distribution may indicate small-world properties of the analyzed network [24].

Network density The neighborhood (n_i) of node i is the set of its neighbors. The connectivity of such a node, denoted by k_i, is the size of its neighborhood. The average number of neighbors indicates the average connectivity of nodes in the network. A normalized version of this parameter is the *network density*, a value between 0 and 1 indicating how densely the network is populated with edges (self-loops and duplicated edges are ignored). A network which contains no edges and solely isolated nodes has a density of 0.

Centralization. The normalized connectivity centralization (also known as degree centralization) is a simple and widely used index of the connectivity distribution.

Network heterogeneity. Many measures of network heterogeneity are based on the variance of the connectivity, and authors differ on how to scale the variance [25]. Describing the heterogeneity (inhomogeneity) of the connectivity (degree) distribution has been the focus of considerable research in recent years [24, 26–28], due to the critical role of 'hub' nodes. Biological networks tend to be very heterogeneous: while some 'hub' nodes are highly connected, the majority of nodes tend to have very few connections.

For the sake of clarifying the above concept we provide in Fig. 3 a *toy network* where the topological parameters can be easily recalculated and fully understood in their physical meaning.

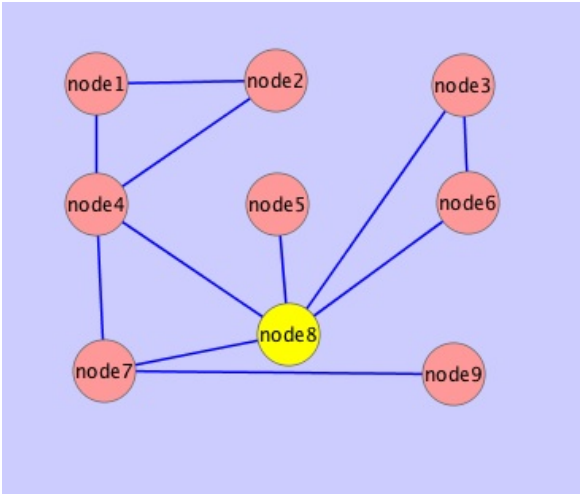

Figure 3: ***Network of a 9-peptide.***
This very simple (toy) network has been generated and analyzed by Cytoscape and one of its plug-in (Network Analyzer), respectively. Notice that the actual 3D (tertiary) structure of the 9-peptide is not appearing in the network representation. Such representation, in fact, points to the significant chemical interactions (links) between residues (nodes), on the only assumption of a minimum threshold distance between nodes. Values of the parameters of the toy network: Clustering coefficient = 0.54; Network diameter = 3; Network radius = 2; Shortest paths = 72; Network centralization = 0.41; Characteristic path length = 2.0; Avg. number of neighbors = 2.44; Network density = 0.31; Network heterogeneity = 0.514.

3 Results

In the present work we decided to explore the heuristic power of the network representation of a 3D protein structure through a quite specific problem, namely the mechanistic details of the $T \rightarrow R$ transition in Hb. The most ambitious goal would have been to pick up the residues involved in the transfer of information between oxygen binding sites, as ultimately responsible of the cooperative, nonliner binding reaction. This is, however, definitely out of range of the typical representation based upon 3D atomic coordinates (even at the highest possible resolution) due to their intrinsically static nature. All in all, the same limitation also applies to the alternative view point focusing on the network of links representative of the changing interactions between residues in the two (R,T) conformations, given the identical source of experimental information the two representations draw on. The topological view point, however, allows a more immediate grasping of the underlying conformational global transition (see below).

PDB	**Edges**	**Nodes**	C_i	**Centralization**	**L(n,m)**	**CPL**	**Density**	**Heterogeneity**
1aj9(α_R)	714	141	0.546	0.043	19740	3.492	0.071	0.264
1gbv(α_T)	717	140	0.545	0.043	19460	3.446	0.073	0.266
1aj9(β_R)	754	145	0.548	0.047	20880	3.537	0.071	0.265
1gbv(β_T)	769	146	0.550	0.046	21170	3.449	0.072	0.284
1aj9$(\alpha\beta)_R$	1526	286	0.527	0.026	81510	4.485	0.037	0.270
1gbv$(\alpha\beta)_T$	1544	287	0.548	0.026	82082	4.493	0.037	0.278

Table 2: *Quantitative descriptors of the protein network used in this work.*
The first column reports the PDB files, concerning the 3D data of R and T conformations of single chains or dimers (in parenthesis). The other columns contain the values of the parameters describing the network topology as provided by Network Analyzer (for their meaning see the text and Figure 3).

We extensively used the ASD database (see the Methods) for a fast and efficient search of structural information concerning the allosteric forms of human Hb, and Table 2 includes in column 1 the PDB data files used as a source of 3D data. Starting from the files representing the T and R forms of haemoglobin, we got two different networks for the α and for the β chains and analyzed thaem by NetworkAnalyzer, a Cytoscape plugin [29]. The network diameter, the average number of neighbors, and the number of connected pairs of nodes as well as the distributions of more complex network parameters such as node degrees, average clustering coefficients, topological coefficients, and shortest path lengths are computed and listed in columns 4-7 of Table 2. In the comparison between T and R states, the former ones appear richer in the number of links for both monomers and dimers (Table 2 column 2). This is in agreement with the more compact structure of the T (tense) conformation. Moreover, from a direct comparison of chains and dimers in the R and T conformations the following points emerge:

1. The β chains appear more sensitive than the α chains to the $R \leftrightarrow T$ switch, as indicated by the higher number of changed edges, higher heterogeneity and longer characteristic path length.

2. The differences between R and T states observed, in the case of dimers, for complex global network descriptors like Characteristic Path Length and Density, are not easily predictable on the basis of the corresponding changes in the isolated α and β monomers. Due to the presence of highly nonlinear interactions, however, this is not in contrast with the critical role assigned to dimers in the transfer of informations within the quaternary structure [17].

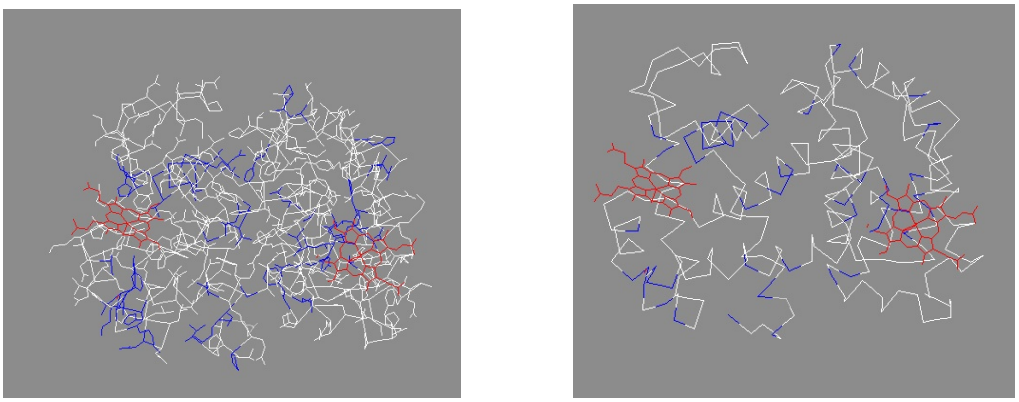

Figure 4: ***Visualizing topological differences in geometrical representations.***
The location of topological differences between R and T forms are visualized in the geometrical structure of the Hb αβ dimers in the R form. The blue residues represent nodes whose number of changes, in terms of (lost/gained) links, is greater than 1; white residues don't change the number of links following the $T \rightarrow R$ switch. The two haemes are shown in red .

Figure 4 shows the locations along the primary structure of the nodes which are more sensitive to the T↔R transition. The red color associated to such nodes is concentrated in the haeme-surrounding regions and at the αβ interface. This is in excellent agreement with, respectively, the motility of F, G and E helices resulting from ligand binding, as indicated in the classical papers by Baldwin and Chotia [30], and the substantial rearrangement of salt-bridge interactions indicated, more than 40 years ago, by M. Perutz as responsible for the cooperative effects between chains within dimers.

In Figure 5 the changing number of links connecting each single residue to its neighbors as a consequence of the T→R switch is provided, taking into account their increase or decrease in terms of positive or negative $T-R$ difference, respectively. Once again, the location of the two residues which are mainly affected by the T→R transition, namely 234 and 168 in the bottom panel of Figure 5, confirms that the β chain is more sensitive to the allosteric change. Moreover, the specific location of such residues in the proximity of the haem is in perfect agreement with the idea that the rearrangements occurring within the haem pockets constitute the actual trigger of the allosteric mechanism.

4 Discussion

Allostery is the most direct and efficient way to regulate the function of a protein, in the frame of homo and heterotropic interactions within the same macromolecule, metabolic control mechanisms, and signal transduction pathways. In addition, disregulation of many allosteric systems have been associated with human diseases like Alzheimer, inflammation and diabetes [31,32]. The most interesting novelty introduced by the topological representation of protein structures lies in the alternative point of view provided on the basis of the same PDB data. To clarify the above statement a very favorable situation is provided by the allosteric changes which have been since a long time studied by 3D distance analysis but only recently reconsidered in a topological perspective [14].

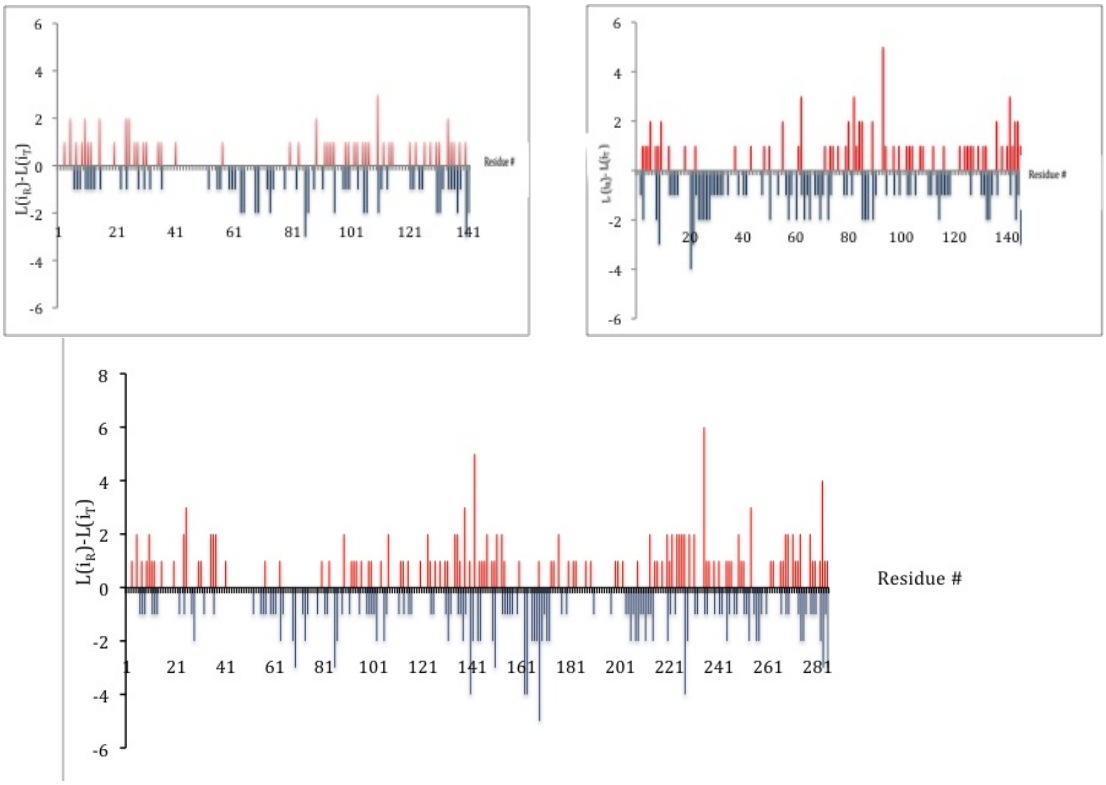

Figure 5: ***T****opological difference between R and T conformations of* α *and* β *Hb chains*
The topological difference between the R and T forms of Hb is visualized in terms of changed links $Li_R - Li_T$ concernig each residue in the sequence of the α and β chains (top left and right panel, respectively) and of the αβ dimer (bottom panel). The horizontal axis marks the residue location in the sequence. In the case of dimers the residue location was calculated chaining, in the order, the α and the β primary structures. The red/blue bars indicate the number of changed links, following the $T \rightarrow R$ switch, in terms of gained/lost links for each single node. For instance, the highest red bar in the bottom panel (αβ dimers), indicates that residues 234 gains 6 links in the $T \rightarrow R$ switch; likewise, the lowest blue bar indicates that residues 168 looses 5 links in the switch.

In this respect it is difficult to overestimate the utility of Figure 4 where the changing landscape of chaemical links between the R and the T conformation are clearly shown within the tertiary structures (left panel) and along the C_α backbone (right panel). However, in order to localize at the level of single residues the topological differences between the two conformations emerging from Table 2, the plots in Figure 5 are even more useful.

Careful consideration of the local link rearrangement along the primary structures shown in Figure 5, in fact, allows: 1) to assess the statistical significance of topological differences, and 2) to identify possible *transition-sensitive loci* other than the haem pocket and the α-β interface. Concerning the first point, at odds with the difficult use of the network global parametsr listed in Table 2, a straightforward t-test (two tails, coupled samples) of the profiles associated to the R and T conformers and coded by the (R-T)/T and (R-T)/R descriptors, produced p-values $<< 0.01$ for all the three panels shown in Figure 5.

As for the second point, it is worth noticing that from Figures 4 and 5, other locations, different from the above mentioned ones, appear sensitive to the $R \leftrightarrow T$ transition. A rationale for that can be found on the basis of the allosteric *heterotropic* (between different sites) interactions causing the Bohr effect in Hb. Similar considerations do not hold in the case of myoglobins, where an analogous phenomenon has been tentatively explained invoking an ancillary enzyme-like function associated to oxygen-storing [14]. In the search for the molecular mechanisms responsible of such observations, the new perspective offered by the topological descriptors of protein structures may reveal precious. In the present case our results, showing a fairly high number of changes in the link profile near the $-NH_2$ terminal residues of both chains (Fig. 5, bottom panel), find an authoritative confirmation in the mechanism suggested by M. Perutz and already mentioned in the result section.

Finally, it should be stressed that what can be observed, at the level of single chains, in terms of links rearrangement ensuing to the $R \leftrightarrow T$ switch (Fig. 5 left and right top panels) is not a perfect mirroring of the corresponding ones at the dimer level (Fig. 5, bottom panel). This is justified by the fact that in the topological representation of monomers the whole set of inter-chain links in dimers are, by necessity, missed. It also represents a further confirmation of the crucial importance of $\alpha\beta$ dimers in the concerted allosteric mechanism of Hb and, on the other hand, it indicates that an exhaustive topological picture of allosteric transitions in Hb cannot miss the information concerning tetramers. As a matter of fact, this will be the subject of our future engagement in the field.

REFERENCES

[1] Monod J., Wyman J., and Changeux J.P. On the nature of allosteric transitions: a plausible model. *J Mol Biol*, 12:88–118, 1965.

[2] Koshland D.E., Nemethy G., and Filmer D. Comparison of experimental binding data and theoretical models in proteins containing subunits. *Biochemistry*, 5:365–385, 1966.

[3] Bellelli A. and Brunori M. Hemoglobin allostery: Variations on the theme. *Biochemica et Biophysica Acta*, 1807:1262–1272, 2011.

[4] Eaton W.A., Henry E.R., Hofrichter J., Bettati S., and Viappiani C.and Mozzarelli A. Evolution of allosteric models for hemoglobin: a critical review. *UBMB Life*, 59(8 9):586 599, August September 2007.

[5] Smith T.J., Schmidt T., Fang J., Wu J., and Siuzdak G. et al. The structure of apo human glutamate dehydrogenase details subunit communication and allostery. *J Mol Biol*, 318:765–777, 2002.

[6] Passner J.M., Schultz S.C., and Steitz T.A. Modeling the camp-induced allosteric transition using the crystal structure of cap -camp at 2.1 a resolution. *J Mol Biol*, 304:847–859, 2000.

[7] Perutz M.F. Stereochemistry of cooperative effects in hemoglobin. *Nature*, 228:726–739, 1970.

[8] Springer T.A. Structural basis for selectin mechanochemistry. *Proc. Natl. Acad. Sci. USA*, 106:91–96, 2009.

[9] Takagi J. and Springer T.A. Integrin activation and structural rearrangement. *Immunol Rev*, 186:141–163, 2002.

[10] Barabási A.L. and Oltvai Z.N. Network biology: understanding the cell's functional organization. . *Nat Rev Genet*, 5:101–113, 2004.

[11] Nussinov R., Tsai C.J., and Csermely P. Allo-network drugs: harnessing allostery in cellular networks. *Trends In Pharmacological Sciences*, (32) (12):686–693, 2011.

[12] Vendruscolo M., Dokholyan N.V., Paci E., and Karplus M. Small-world view of the amino acids that play a key role in protein fold. *Phys Rev*, 65:06191010619104, 2002.

[13] Amitai G., Shemesh A., Sitbon E., Shklar M., Netanely D., Venger I., and Pietrokovski S. Network analysis of protein structures identifies functional residues. *J Mol Biol*, 344:11351146, 2004.

[14] del Sol A., Fujihashi H., Amoros D., and Nussinov R.. Residues crucial for maintaining short paths in network communication mediate signaling in proteins. *Molecular Systems Biology*, page 112, 2006.

[15] De Ruvo M., Giuliani A., Santori D., and Di Paola L. Shedding light on protein-ligand binding by graph theory: the topological nature of allostery. *Biophysical Chemistry*, 2012.

[16] Huang Z., Zhu L., Cao Y., Wu G., Liu x., Chen Y., Wang Q., Zhao T.S.Y., Wang Y., Li W., Li Y., Chen H., Chen G., Zhang J., et al. Asd: a comprehensive database of allosteric proteins and modulators. *Nucleic Acids Research*, 39:663–669, 2011.

[17] Perutz M.F. Nature of haem-haem interaction. *Nature*, 237:495–499, 1972.

[18] Martin A.J.M., Vidotto M., Boscariol F., Di Domenico T., Walsh I., and Tosatto S.C.E.. Ring: Networking interacting residues, evolutionary information and energetics in protein structures. *Bioinformatics,*, 2011.

[19] Smoot M., Keiichiro O., Ruscheinski J., Wang P.L., and Ideker T.. Cytoscape 2.8: new features for data integration and network visualization. *Bioinformatics,*, 27(3):431–432, 2011.

[20] Cline M.S., Smoot M., Cerami E., Kuchinsky A., Landys N., Workman C., Christmas R., Avila-Campilo I., Creech M., and Gross B. et al. Integration of biological networks and gene expression data using cytoscape. *Nature Protocols*, 2:2366–2382, September 2007.

[21] Shannon P., Markiel A., Ozier O., Baliga N.S., Wang J.T., Ramage D., Amin N., Schwikowski B., and Ideker T. Cytoscape: a software environment for integrated models of biomolecular interaction networks. *Genome Research*, 13(11):2498–504, November 2003.

[22] Bollobas B. *Random graphs*. Cambridge University Press, Cambridge, 2001.

[23] Estrada. Universality in protein structure networks. *Biophysical Journal*, 98 (5)::890–900, 2010.

[24] Watts D.J. and Strogatz S.H. Collective dynamics of 'small-world' networks. *Nature*, 393:440–442, 1998.

[25] Ravasz E. et al. Hierarchical organization of modularity in metabolic networks. *Science*, 297:1551–1555, 2002.

[26] Dong J. and Horvath S. Understanding network concepts in modules. *BMC Syst Biol*, 24, 2007.

[27] Tanaka R., Yi T.M, and Doyle J. Some protein interaction data do not exhibit power law statistics. *FEBS Letters*, 579:5140–5144, 2005.

[28] Weisstein E. W. Least squares fitting - power law. *MathWorld - A Wolfram Web Resource.(http://mathworld.wolfram.com/LeastSquaresFittingPowerLaw.html)*, 1990.

[29] Assenov Y., Ramírez F., Schelhorn S.E., Lengauer T., and Albrecht M. Computing topological parameters of biological networks. *Bioinformatics,*, 24(2):282–284, 2008.

[30] Baldwin J.M. and Chothia C.. Haemoglobin: the structural changes related to ligand binding and its allosteric mechanism. *J. Molecular Biology*, 129(2):175–220, 1979.

[31] Dickerson R.E. and Geis I. *Hemoglobin: Structure, Function, Evolution, and Pathology,*. Benjamin / Cummings, Menlo Park , CA, 1983.

[32] Noinaj N., Bhasin S.K., Song E.S., Scoggin K.E., Juliano M.A., Juliano L., Hersh L.B., and Rodgers D.W. Identification of the allosteric regulatory site of insulysin. *Plos One*, 6:1–11, 2011.